Available online at www.sciencedirect.com
ScienceDirect
Journal of Sound and Vibration 322 (2009) 665–673
JOURNAL OF SOUND AND VIBRATION
www.elsevier.com/locate/jsvi

Causal semiactive control of seismic response

U. Aldemir*

Faculty of Civil Engineering, Division of Applied Mechanics, Istanbul Technical University, 34469 Maslak, Istanbul, Turkey

Received 3 April 2008; received in revised form 5 October 2008; accepted 1 December 2008
Handling Editor: C.L. Morfey
Available online 13 January 2009

Abstract

A challenge in the use of semiactive dampers for the earthquake response reduction is the development of implementable control algorithms. Exact optimal control resulting from the numerical solution to Euler–Lagrange equations requires a priori knowledge of earthquake in the control interval, which is not possible. This paper proposes a causal sub-optimal implementable control to reduce the earthquake response using an inherently nonlinear controllable fluid damper. The proposed method is basically based on the prediction of the near-future ground accelerations using maximum-entropy method. The earthquake response of low-rise, two degree of freedom (dof) base isolated structure is investigated for the proposed causal sub-optimal control and the resulting performance is compared to the exact optimal control and the uncontrolled case. The results show that the proposed control is promising in protecting the earthquake-excited buildings.

1. Introduction

The strong desire for better utilization of new materials and lower costs have motivated the development of new concepts for protecting structures from earthquakes. Passive and active control techniques have already been widely studied to alleviate the seismic hazards in civil engineering structures [1–11]. Among the passive systems, base isolation is one of the most effective and widely-used systems because of its simple mechanism and cost. These systems use a flexible isolation system implemented between the foundation and the superstructure so as to increase the natural period of the structure. However, some researchers [12–15] have recently raised concerns as to its efficiency considering the near-fault, high-velocity, long-period seismic pulses, which may cause large isolation displacements at isolation period. The large displacement requirements of isolation bearings have resulted in solution, which is not economically feasible. The use of supplemental dampers in seismic isolation reduces the base isolator displacements, but can have the undesirable effect of increasing interstory displacements and accelerations in the superstructure for high levels of damping [13]. An increase in the interstory drifts and superstructure accelerations is counter to the primary goal of isolation systems: to protect the sensitive internal equipment and non-structural elements. Makris [16] illustrated the solution to this problem as to use an adaptive damping system like semiactive damping system.

*Tel.: +90 212 285 37 08; fax: +90 212 285 65 87.
E-mail address: aldemiru@itu.edu.tr

0022-460X/$ - see front matter © 2008 Elsevier Ltd. All rights reserved.
doi:10.1016/j.jsv.2008.12.002

The recent developments have shown that the semiactive dampers are promising in suppressing the vibrations [17–22]. Semiactive control systems are a class of control systems in which the control actions are applied by changing the mechanical properties (i.e., stiffness and damping) of the control device with almost no external power. A challenge in the use of semiactive dampers is the development of implementable nonlinear control algorithms. The most general approach for solving optimal control problems for nonlinear systems requires the solution of a two-point boundary value problem described by Euler–Lagrange equations via numerical dynamic optimization techniques [14,23,24]. Since these techniques require a priori knowledge of earthquake excitation, the resulting optimal control is non-implementable and is useful to check the optimality of implementable causal control strategies. Some recent studies on the development of causal nonlinear strategies for structures incorporating semiactive devices have been given in Refs. [25–29].

In this study, seismic response of a two degree of freedom (dof) low-rise base isolated structure with a controllable fluid damper installed at isolation level has been investigated for uncontrolled, proposed sub-optimal and exact optimal control cases. Sub-optimal control has been obtained using the 10-step ahead near-future predictions of ground accelerations while the exact optimal control has been derived from the numerical solution to the Euler–Lagrange equations using the a priori knowledge of excitation in the whole control interval. The numerical solution to the Euler–Lagrange equations has been obtained using a gradient approach in which the state and the costate equations have been solved based on the successive iterations made on the control trajectory. The performance of the proposed sub-optimal control has been compared to the uncontrolled case and the exact optimal control case.

2. Structural system

The base isolation system used in this study is assumed to be linear and represented by a linear spring in parallel with a linear viscous dash-pot. The masses m_s and m_i represent the superstructure of the building and the mass of the base floor above the isolation system, respectively. The superstructure and the isolation stiffness and damping coefficients are represented by k_s, c_s, k_i and c_i, respectively. Structural relative displacements and the ground displacement are denoted by r_1, r_2 and z, respectively. For the example structure; the masses, the stiffness and the damping coefficients are selected as $m_i = m_s = 10^5\,\mathrm{kg}$, $k_i = 1.65 \times 10^6\,\mathrm{N\,m^{-1}}$, $k_s = 3 \times 10^7\,\mathrm{N\,m^{-1}}$, $c_i = 1.1 \times 10^5\,\mathrm{N\,s\,m^{-1}}$ and $c_s = 3 \times 10^4\,\mathrm{N\,s\,m^{-1}}$ [14]. The controllable damper implemented in the isolation level (Fig. 1) is modeled by the following algebraic expression with five parameters:

$$f = f_0 u H(u) \tanh(r_1/d_0 + \dot{r}_1/v_0) + k_d r_1 + c_d \dot{r}_1 \tag{1}$$

where the constant parameters d_0 and v_0 are used to describe the pre-yield behavior of the device, f_0 is a controllable yield force, and k_d and c_d describe the post-yield behavior and the behavior when $u = 0$. The control force f is changed optimally via the control decision variable u; $H(u)$ is the Heaviside step function of u.

As briefly stated in introduction, there are mainly two types of semiactive control systems: (a) active variable stiffness and (b) active variable damping. In active variable stiffness application, the structural stiffness is modified to achieve a non-resonant condition between the response and the excitation. In the active variable

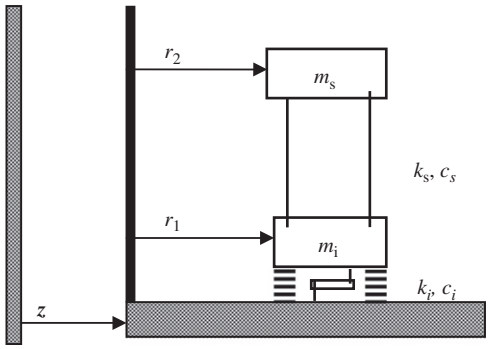

Fig. 1. Idealized model for a two DOF (degree-of-freedom) base isolated structure.

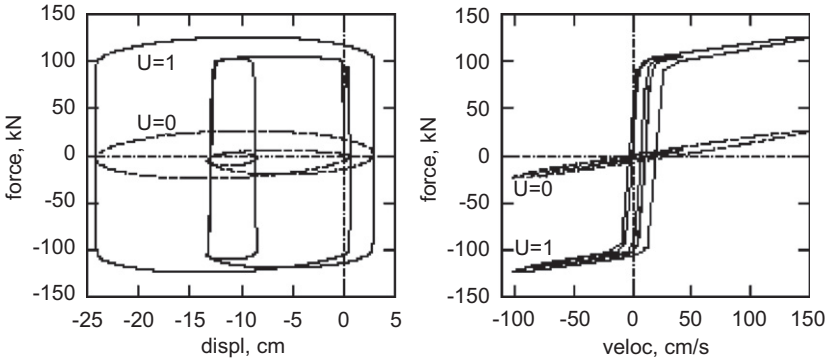

Fig. 2. Hysteretic behavior of the controllable damper for $u = 0$ and 1.

damping application, supplemental energy dissipation devices such as friction and fluid dampers are modified to allow adjustments in their damping capacities. Eq. (1) can represent the electro-rheological (ER) dampers, magneto-rheological (MR) dampers and also fluid dampers. Device parameters used are $f_0 = 10^5\,\mathrm{N}$, $d_0 = 0.05\,\mathrm{m}$, $v_0 = 0.04\,\mathrm{m\,s^{-1}}$, $c_d = 2\times10^5\,\mathrm{N\,s\,m^{-1}}$ and $k_d = 3\times10^5\,\mathrm{N\,m^{-1}}$. These constant parameters in Eq. (1) are selected to represent the behavior of controllable dampers [30,31]. The inherent device stiffness is very small compared to structural stiffness. The dominant contribution of the device to structural response is through the damping. This contribution can also be seen from Fig. 2, which shows the hysteretic behavior of the investigated semiactive damper modeled by Eq. (1) for $u = 0$ and $u = 1$. The proposed control defined in Section 4 modifies the energy dissipation capacity of the structure via the controllable fluid damper (semiactive damping device) based on a sub-optimal control policy.

3. Exact optimal control

The exact optimal control is derived from the numerical solution to the Euler–Lagrange equations. Since the detailed derivation of Euler–Lagrange equations can be found in Ref. [23], only the results will be given here. A general nonlinear system of dynamical equations, subjected to control actions $\mathbf{u}(t)$ and with initial conditions $\mathbf{x}_0$ is

$$\dot{\mathbf{x}}(t) = \mathbf{f}(\mathbf{x}(t), \mathbf{u}(t), t); \quad \mathbf{x}(t_0) = \mathbf{x}_0, \ \ \mathbf{x} \in R^n, \ \ \mathbf{u} \in R^m \tag{2}$$

The optimal control strategy $\mathbf{u}(t)$ minimizes the integral cost function J,

$$J = \int_0^{t_f} L(\mathbf{x}(t), \mathbf{u}(t), t)\,\mathrm{d}t \tag{3}$$

where $L(\mathbf{x},\mathbf{u},t)$ is the scalar Lagrangian of the cost function. The Hamiltonian H is defined as

$$H(\mathbf{x}(t), \mathbf{u}(t), \boldsymbol{\lambda}(t), t) = L(\mathbf{x}(t), \mathbf{u}(t), t) + \boldsymbol{\lambda}^{\mathrm{T}}\mathbf{f}(\mathbf{x}(t), \mathbf{u}(t), t) \tag{4}$$

where $\boldsymbol{\lambda}(t)$ is the costate vector. The Euler–Lagrange equations provide the necessary conditions for optimality [23]:

$$\dot{\boldsymbol{\lambda}}(t) = \left(-\frac{\partial H}{\partial \mathbf{x}}\right)^{\mathrm{T}} = -\left[\frac{\partial \mathbf{f}(\mathbf{x},\mathbf{u},t)}{\partial \mathbf{x}}\right]^{\mathrm{T}}\boldsymbol{\lambda}(t) - \left[\frac{\partial L(\mathbf{x},\mathbf{u},t)}{\partial \mathbf{x}}\right]^{\mathrm{T}}, \quad \boldsymbol{\lambda}(t_f) = \mathbf{0} \tag{5}$$

$$\frac{\partial H}{\partial \mathbf{u}} = \boldsymbol{\lambda}^{\mathrm{T}}(t)\frac{\partial \mathbf{f}(\mathbf{x},\mathbf{u},t)}{\partial \mathbf{u}} + \frac{\partial L(\mathbf{x},\mathbf{u},t)}{\partial \mathbf{u}} = \mathbf{0} \tag{6}$$

Eqs. (2) and (5) define a two-point boundary value problem. Simultaneous solution of these coupled state and costate equations throughout the control interval can be difficult for non-autonomous systems. In this paper, a gradient

approach in which iterations are made on the control function $\mathbf{u}(t)$ is used based on the update equation

$$\mathbf{u}_{k+1}(t) = \mathbf{u}_k(t) + K_k \frac{\partial H(\mathbf{x}, \mathbf{u}, t)}{\partial \mathbf{u}} \tag{7}$$

where K_k is a scalar gradient gain.

For the purpose of obtaining the optimal solutions, the nonlinear system of dynamical equation of a two dof base isolated structure with the selected semiactive damper can be expressed as

$$\dot{\mathbf{x}}(t) = \mathbf{f}(\mathbf{x}(t), u(t), t) = \mathbf{A}\mathbf{x} + \mathbf{g}(\mathbf{x}, u)u + \mathbf{G}\ddot{z}(t), \quad \mathbf{x}(t_0) = \mathbf{0} \tag{8}$$

where

$$\mathbf{x} = \begin{Bmatrix} r_1 \\ r_2 \\ \dot{r}_1 \\ \dot{r}_2 \end{Bmatrix}; \quad \mathbf{A} = \begin{bmatrix} 0 & 0 & 1 & 0 \\ 0 & 0 & 0 & 1 \\ -\dfrac{k_i + k_s + k_d}{m_i} & \dfrac{k_s}{m_i} & -\dfrac{c_i + c_s + c_d}{m_i} & \dfrac{c_s}{m_i} \\ \dfrac{k_s}{m_s} & -\dfrac{k_s}{m_s} & \dfrac{c_s}{m_s} & -\dfrac{c_s}{m_s} \end{bmatrix} \tag{9}$$

$$\mathbf{g}(\mathbf{x}, u) = \begin{Bmatrix} 0 \\ 0 \\ -(f_0/m_i)H(u)\ \tanh(r_1/d_0 + \dot{r}_1/v_0) \\ 0 \end{Bmatrix}; \quad \mathbf{G} = \begin{Bmatrix} 0 \\ 0 \\ -1 \\ -1 \end{Bmatrix} \tag{10}$$

The cost function J to be minimized is selected as

$$J = \int_{t_0}^{t_f} L(\mathbf{x}(t), u(t), t)\,\mathrm{d}t = \int_{t_0}^{t_f} [\ddot{r}_2(t) + \ddot{z}(t)]^2\,\mathrm{d}t = \int_{t_0}^{t_f} \left\{ \frac{k_s[r_2(t) - r_1(t)] + c_s[\dot{r}_2(t) - \dot{r}_1(t)]}{m_s} \right\}^2 \mathrm{d}t \tag{11}$$

where the Lagrangian $L(\mathbf{x}(t), u(t), t)$ is the square of the superstructure absolute acceleration. To initialize the previously defined iterative solution procedure, the control trajectory $u(t)$ is selected as $u_{k=0}(t) = 1$ in the control interval and the final time t_f for the cost function is equal to the earthquake duration.

4. Sub-optimal control based on prediction of near-future excitation

As stated in the previous section, exact optimal value of the control variable $u(t)$ at time t resulting from the numerical solution to Euler–Lagrange equations requires a priori knowledge of ground excitations in the control interval. Even though a priori knowledge of ground excitations in the whole control interval is not possible in practice, the current excitation at time t can be measured and feed back to the system instantaneously for control purposes [7]. Moreover, near-future ground accelerations can be predicted using various prediction algorithms [2,32–34]. Provided that the current ($\ddot{z}(\tau = t)$) and the near-future ground accelerations ($\ddot{z}_i(\tau = t + i\Delta t)$, $i = 1, 2, 3, \ldots, N$) are available by measurement and prediction at the current time t, the numerical solution to Euler–Lagrange equations can be obtained as given in the previous section for the sub-interval $[t, t + N\Delta t]$ in which the accelerations are predicted, instead of whole control interval.

Since the Euler–Lagrange equations are solved in the sub-interval including the predicted ground accelerations, the resulting control will be sub-optimal, which refers to the approximately optimal solution and denoted by $u_{so}(\tau)$, $t \leqslant \tau \leqslant t + N\Delta t$. To initialize iterative solution procedure, the sub-optimal control trajectory $u_{so}(\tau)$ is selected as $u_{so}(\tau) = 1$, $t \leqslant \tau \leqslant t + N\Delta t$ while the final time $(t_f)_{so}$ for the cost function is equal to $(t_f)_{so} = t + N\Delta t$ where $\Delta t = 0.005$ s is the sampling time for the El Centro-NS earthquake and N, the number of ground acceleration to be predicted, which is selected as 10 in this study.

Namely, the sub-optimal control trajectory $u_{so}(\tau)$ minimizes the integral cost function

$$J_{so} = \int_{t}^{t+N\Delta t} L(\mathbf{x}(\tau), u_{so}(\tau), \tau)\,\mathrm{d}\tau \tag{12}$$

Once the sub-optimal control trajectory $u_{so}(\tau)$ is obtained for the sub-interval $[t, t+N\Delta t]$, $u_{so}(\tau = t)$ is the value of the control variable, which must be applied to the controllable damper. Then, the next N near-future ground accelerations are predicted for the next optimization interval and the corresponding Euler–Lagrange equations are solved and the control process continues in this way.

Proposed technique has been also applied to linear structures by the author and his coauthors [2–4]. In those studies, the problem is relatively simpler since the investigated structures are linear so that the state and costate equations are decoupled. However, the state and costate equations are generally coupled in the nonlinear systems as in this case.

Since the detailed derivation of the prediction algorithm maximum-entropy method (MEM) for the near-future ground accelerations ($\ddot{z}_i(\tau = t + i\Delta t)$, $i = 1, 2, 3, \ldots, N$) can be found in literature, only the results will be given here for the completeness of the paper [32,33]. Earthquake motion can be modeled as a q-dimensional autoregressive (AR) process, which is specified by

$$g_t = \mathbf{S}_{t-1}\mathbf{a} + v_t \tag{13}$$

where the time varying matrix $\mathbf{S}_{t-1}$ and the parameter vector $\mathbf{a}$ are given by

$$\mathbf{S}_{t-1} = [-g_{t-1}, -g_{t-2}, \ldots, -g_{t-q}] \tag{14}$$

$$\mathbf{a} = [a_1, a_2, \ldots, a_q] \tag{15}$$

State–space form of the AR model parameters can be described as

$$\mathbf{a}_t = \mathbf{I}\mathbf{a}_{t-1} \tag{16}$$

A fast and simple recursion procedure for MEM spectral estimation was proposed by Andersen [33]. This procedure is just a formalization based on the method given by Burg [32]. Useful recursion formulas for the estimation of AR model parameters a_{mn} are given as

$$a_{mn} = a_{m-1,k} - a_{m,m}a_{m-1,m-k}, \quad k = 1, \ldots, m-1 \tag{17}$$

$$a_{m,m} = 2\sum_{t=1}^{N-m} b_{m,t}b^*_{m,t} \Bigg/ \sum_{t=1}^{N-m} (b_{m,t})^2 (b^*_{m,t})^2 \tag{18}$$

$$b_{m,t} = b_{m-1,t} - a_{m-1,m-1}b^*_{m-1,t} \tag{19}$$

$$b^*_{m,t} = b^*_{m-1,t+1} - a_{m-1,m-1}b_{m-1,t+1} \tag{20}$$

where $a_{m,k}$ expresses the kth parameter on m-dimensional AR model and N, the number of data to be used for the identification. The initial conditions for Eqs. (17)–(20) are given as

$$b_{1,t} = x_t, b^*_{1,t} = x_{t+1}, \quad t = 1, \ldots, N-1 \tag{21}$$

where x_t denotes equally spaced ground acceleration data at time t. The real value of the ground acceleration at time t can be measured on line while the other $N-1$ data can be assumed to start the prediction process. They may even be assumed to be almost equal to x_t which is the only data available. However, we will have all the real-measured values of ground acceleration after N steps later and continue to prediction using the measured real data.

MEM is used for the parameter estimation of AR process, which describes the ground motion. It is supposed that the parameters at time t are obtained by using the available information from $(t-N\Delta t)$ to t. For this purpose, Eqs. (17)–(20) are repeated under the initial conditions given by Eq. (21) until m is equal to the order of the AR model. Selection of the amount of information (N) for the identification and the model order is usually ambiguous. However, the order of AR model for earthquake ground motions is generally selected between two and five [34]. So in this study two-dimensional AR model is selected.

Once the parameters are estimated, the predictions at time $t+1$ and $t+i$ are evaluated by using the following equations:

$$\hat{g}_{t+1} = \mathbf{S}_t \hat{\mathbf{a}}_{t+1|t} \tag{22}$$

$$\hat{g}_{t+1+i} = \mathbf{S}_{t+i} \hat{\mathbf{a}}_{t+1|t} \tag{23}$$

where $\mathbf{S}(t+i)$ is given by

$$\mathbf{S}_{t+i} = [-\hat{g}_{t+i}, -\hat{g}_{t+i-1}, \ldots, -g_t, -g_{t-1}, \ldots, -g_{t+i-q+1}] \tag{24}$$

It must be noted here that the primary focus of this study is not on the analysis of the prediction algorithm. It is also beyond the scope of this paper how the performance of the control algorithm has been affected by the number of prediction steps. Some of these issues have been studied in Refs. [2–4] for linear structures. The prediction of near-future seismic data is not the contribution of this study since it has already been studied in literature using different techniques. The main contribution of this study is the proposed new, sub-optimal implementable control rule, which uses the prediction of near-future ground accelerations in conjunction with the solution of Euler–Lagrange equations.

5. Numerical results

Seismic response of two dof low-rise base isolated structure with a controllable fluid damper under the May 18, 1940 Imperial Valley earthquake El Centro (NS component) (Fig. 3) is evaluated in order to examine the performance of the proposed control in comparison to uncontrolled case and the exact optimal case.

The calculations are performed for the first 10 s-duration of the excitation, which includes the peak acceleration values. The damper force is zero for the uncontrolled case. The damper forces for the proposed sub-optimal and exact optimal control are given in Fig. 4. As shown in Fig. 4, the damper force governed by the sub-optimal control $u_{so}(\tau)$, $t \leqslant \tau \leqslant t + N\Delta t$ follows the damper force governed by the exact optimal control $u(t)$, $0 \leqslant t \leqslant t_f$ except for the peak values. Proposed sub-optimal damper force is generally smaller in magnitude than the exact optimal damper force. Since the proposed sub-optimal and exact optimal control algorithms use the same semiactive damper, the resulting damper force levels are directly related to the selected control algorithm. The peak damper forces required by exact optimal control are dependent on the structural properties and the characteristics of the ground motion. The exact optimal control trajectory may require very large control forces for large near-field earthquakes which may be difficult to achieve in practice [17].

Time histories for the response (interstory displacement and the superstructure absolute acceleration) and the cost functions are illustrated in Fig. 5 for all the investigated cases. The maximum values are also given in Table 1. As indicated in Fig. 5 and Table 1, the uncontrolled cost function is the maximum and the exact

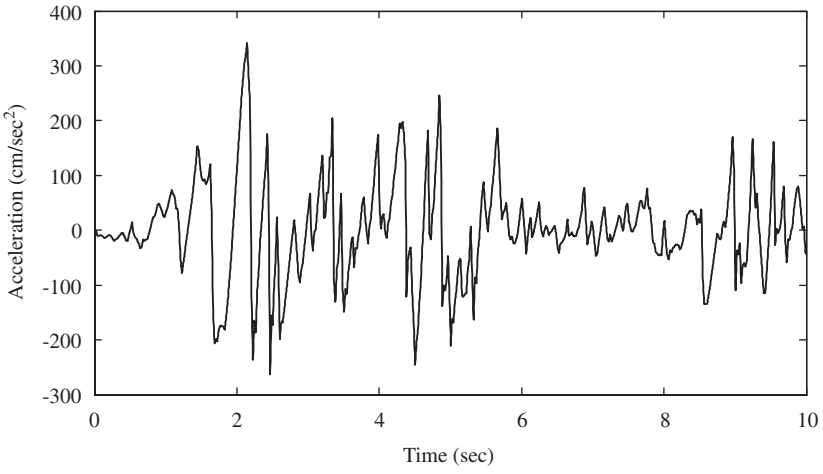

Fig. 3. May 18, 1940 Imperial Valley earthquake El Centro (NS component).

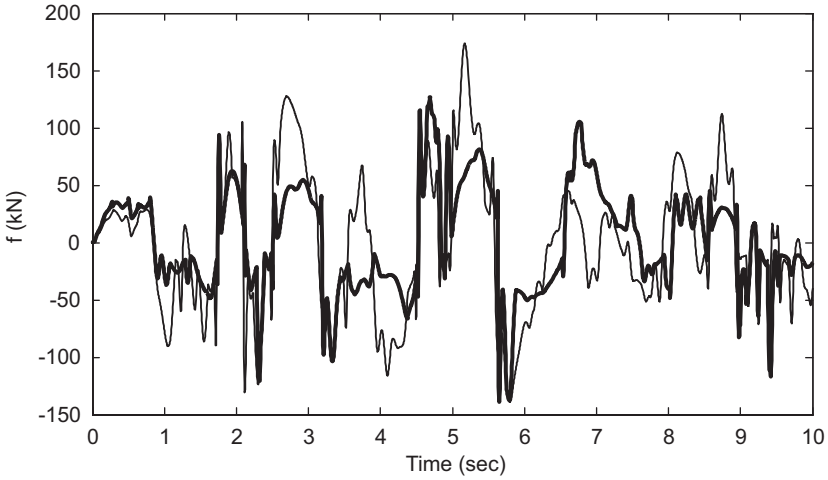

Fig. 4. Damper forces; sub-optimal (thick) and exact optimal (thin).

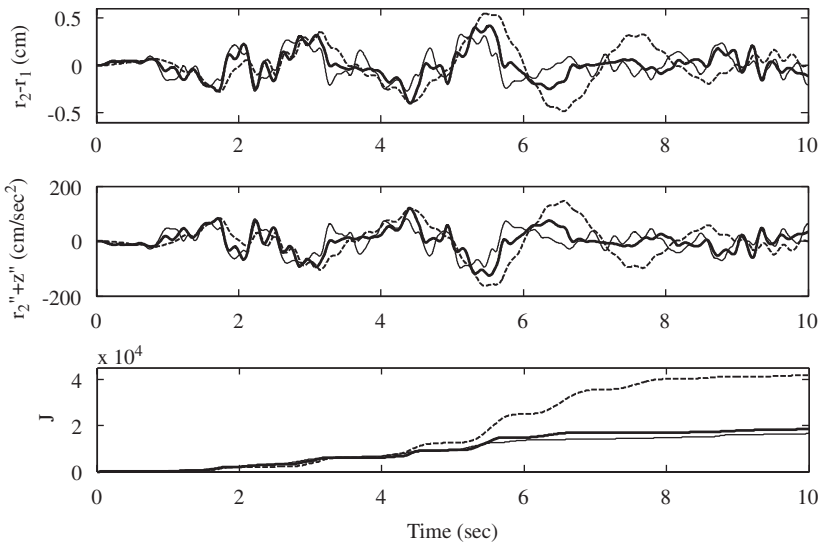

Fig. 5. Comparison of sub-optimal (thick) to uncontrolled (dashed) and exact optimal (thin).

Table 1
Maximum response quantities for uncontrolled and controlled cases.

Maximum values	Uncontrolled	Sub-optimal control	Exact optimal control
r_2-r_1 (cm)	0.54	0.42	0.30
$\ddot{r}_2(t)+\ddot{z}(t)$ (cm/s^2)	163.10	125.50	97.50
J	41 671	18 439	16 579

optimal cost function is the minimum while the proposed sub-optimal cost function is just between them for $t_f = 10$ s. It is clear from Fig. 5 that the sub-optimal cost function is much smaller than the uncontrolled cost function. It is shown that the proposed sub-optimal control policy is very significant in suppressing the uncontrolled interstory displacement and the superstructure absolute acceleration. Fig. 5 also shows that sub-optimal response and cost trajectories follow closely the exact optimal response and cost trajectories except for

peak values even though proposed sub-optimal control uses only the 10-step ahead ground acceleration predictions. It is expected that as we predict the more distant future ground accelerations more accurately, the performance of the proposed sub-optimal control will approach to the performance of the exact optimal control. These analyses show that the proposed sub-optimal control is promising for the control of earthquake response of structures.

6. Conclusion

Exact optimal control resulting from the numerical solution to Euler–Lagrange equations is an idealized case and can not be implemented since it requires a priori knowledge of earthquake in the control interval. In this study, a new sub-optimal implementable control rule, which uses the prediction of near-future ground accelerations, has been proposed. To evaluate the performance of the proposed control, the real-time control of a two degree of freedom (dof) low-rise base isolated structure with a controllable fluid damper under earthquake excitation has been investigated and the corresponding results have been compared to uncontrolled and exact optimal control cases. Numerical results show that the proposed sub-optimal control is very effective in reducing the uncontrolled earthquake response and is promising for implementation since it results in solutions close enough to exact optimal solutions in terms of the reduction in the cost function and super structure response.

Acknowledgments

The author gratefully acknowledges the support from the European Commission for "*FP6*, *LessLoss-Risk Mitigation for Earthquakes and Landslides*" (http://www.lessloss.org/main/index.php, Contract no: GOCE-CT-2003-505448) and thanks M. Ozdilim for his help in evaluating the simulations.

References

[1] J. Park, D. Reed, Analysis of uniformly and linearly distributed mass dampers under harmonic and earthquake excitation, *Engineering Structures* 23 (7) (2001) 802–814.
[2] M. Bakioglu, U. Aldemir, A new numerical algorithm for sub-optimal control of earthquake excited structures, *International Journal for Numerical Methods in Engineering* 50 (2001) 2601–2616.
[3] U. Aldemir, M. Bakioglu, Active control based on the prediction and degree of stability, *Journal of Sound and Vibration* 247 (4) (2001) 561–576.
[4] U. Aldemir, M. Bakioglu, S.S. Akhiev, Optimal control of linear structures, *Earthquake Engineering & Structural Dynamics* 30 (6) (2001) 835–851.
[5] S.K. Rasouli, M. Yahyai, Control of response of structures with passive and active tuned mass dampers, *Structural Design of Tall Buildings* 11 (1) (2002) 1–14.
[6] B. Yoo, Y.H. Kim, Study on effects of damping in laminated rubber bearings on seismic responses for a 1/8 scale isolated test structure, *Earthquake Engineering & Structural Dynamics* 31 (10) (2002) 1777–1792.
[7] S.S. Akhiev, U. Aldemir, M. Bakioglu, Multipoint instantaneous optimal control of structures, *Computers & Structures* 80 (2002) 909–917.
[8] P. Tan, L. Tong, D.C. Sun, Dynamic characteristics of a beam system with active piezoelectric fiber reinforced composite layers, *Composites Part B—Engineering* 33 (7) (2002) 545–555.
[9] P. Tan, L. Tong, A one-dimensional model for non-linear behavior of piezoelectric composite materials, *Composite Structures* 58 (2002) 551–561.
[10] A.K. Agrawal, P. Tan, S. Nagarajaiah, J. Zhang, Development of a Benchmark structural control model for a highway bridge, *Proceedings of the Fourth International Workshop on Structural Control*, New York, USA, 2004, pp. 9–11.
[11] P. Tan, S.J. Dyke, R. Andy, A. Makola, Integrated device placement and control design in civil structures using genetic algorithms, *Journal of Structural Engineering* 131 (10) (2005) 1489–1496.
[12] J.M. Kelly, The role of damping in seismic isolation, *Earthquake Engineering & Structural Dynamics* 25 (1999) 3–20.
[13] R.S. Jangid, J.M. Kelly, Base isolation for near-fault motions, *Earthquake Engineering & Structural Dynamics* 30 (5) (2001) 691–707.
[14] U. Aldemir, H.P. Gavin, Optimal semiactive control of structures with isolated base, *International Applied Mechanics* 42 (2) (2006) 235–240.
[15] R.S. Jangid, Optimum lead–rubber isolation bearings for near-fault motions, *Engineering Structures* 29 (2007) 2503–2513.
[16] N. Makris, Rigidity–plasticity–viscosity: can electrorheological dampers protect base-isolated structures from near-source ground motions?, *Earthquake Engineering & Structural Dynamics* 26 (5) (1997) 571–591.

[17] H.P. Gavin, U. Aldemir, Optimal control of earthquake response using semiactive isolation, *Journal of Engineering Mechanics* 8 (2005) 769–776.
[18] Y. Choi, N.M. Wereley, Biodynamic response mitigation to shock loads using magnetorheological helicopter crew seat suspensions, *Journal of Aircraft* 42 (5) (2005).
[19] H.P. Gavin, A. Zaicenco, Performance and reliability of semi-active equipment isolation, *Journal of Sound and Vibration* 306 (2007) 74–90.
[20] X. Song, M. Ahmedian, S.C. Southward, Analysis and strategy for superharmonics with semiactive magneto-rheological suspension systems, *ASME Journal of Dynamic Systems, Measurement and Control* 129 (6) (2007) 795–803.
[21] X. Song, M. Ahmedian, S.C. Southward, L. Miller, Parametric study of nonlinear adaptive control algorithm with magneto-rheological suspension systems, *Communications in Nonlinear Science and Numerical Simulation* 12 (4) (2007) 584–607.
[22] S.B. Choi, J.H. Choi, Y.S. Lee, M.S. Han, Vibration control of an ER seat suspension for a commercial vechile, *ASME Journal of Dynamic Systems, Measurement and Control* 125 (2007) 60–68.
[23] R.F. Stengel, *Optimal Control and Estimation*, Dover, New York, 1994.
[24] U. Aldemir, Optimal control of structures with semiactive tuned mass dampers, *Journal of Sound and Vibration* 266 (4) (2003) 847–874.
[25] G. Leitmann, E. Reithmeier, Semiactive control of a vibrating system by means of electrorheological fluids, *Dynamics and Control* 3 (1) (1993) 7–33.
[26] S.J. Dyke, B.F. Spencer, M.K. Sain, J.D. Carlson, Modeling and control of magnetorheological dampers for seismic response reduction, *Smart Materials and Structures* 5 (1996) 565–575.
[27] H. Yoshioka, J.C. Ramallo, B.F. Spencer, Smart base isolation strategies employing magnetorheological dampers, *Journal of Engineering Mechanics* 128 (5) (2002) 540–551.
[28] J.C. Ramallo, E.A. Johnson, B.F. Spencer, Smart base isolation systems, *Journal of Engineering Mechanics* 128 (10) (2002) 1088–1099.
[29] Z.G. Ying, W.Q. Zhu, A stochastic optimal semi-active control strategy for ER/MR dampers, *Journal of Sound and Vibration* 259 (1) (2003) 45–62.
[30] H.P. Gavin, M. Dobossy, C. Lamberton, Designing and testing devices for semi-active structural control, *Proceedings of the Third International Workshop on Structural Control*, Paris, France, 2000, pp. 255–262.
[31] H.P. Gavin, Multi-duct electrorheological dampers, *Journal of Intelligent Materials and Structures* 12 (5) (2001) 353–366.
[32] J.P. Burg, The relationship between the maximum entropy spectra and maximum likelihood spectra, *Geophysics* 37 (1967) 375–376.
[33] N. Andersen, On the calculation of filter coefficient for maximum entropy analysis, *Geophysics* 39 (1974) 69–72.
[34] M. Hoshiya, O. Maruyama, Adaptive identification of autoregressive processes, *ASCE Journal of Engineering Mechanics* 117 (7) (1991) 442–454.